The U.S. GOVERNMENT

IS ABSOLVED

FROM ANY LITIGATION WHICH MAY ENSUE FROM THE CONTRACTORS IN-FRINGING ON THE FOREIGN PATENT RIGHTS WHICH MAY BE INVOLVED.

WRIGHT FIELD, DAYTON, OHIO

REEL – C

150

6212

8960

F.M. 842
Perf.47
0.523

8960

F.M. 842
Perf.47
0.523

FLUID MOTION SUB-COMMITTEE

AERONAUTICAL RESEARCH COUNCIL

Tests of a Double Wedge Aerofoil with a 30 per cent Control Flap over a Range of Supersonic Speeds

- By -
F. W. Pruden, B.Sc.,
of the Aerodynamics Division, N.P.L.

8th September, 1945

Summary

Supersonic tests were carried out on a two dimensional symmetrical double wedge aerofoil 6 per cent thick with a 30 per cent control flap set at 4 deg. and 0 deg., two separate models being used. The first model was also tested with the trailing edge foremost.

Lift, drag and pitching moment were measured over a range of Mach numbers from 1.16 to 1.45.

The results agree reasonably with Busemann theory as detailed by Lock[2] over the range in which the theory applies, breakdown of the theory tending to occur for sufficiently low Mach numbers and high incidences. Discrepancies between observation and theory tend to increase as the point of breakdown of the theory is approached. They may be tentatively attributed to tunnel interference and bad velocity distribution in the empty tunnel; breakaway near the trailing edge may also contribute.

It was concluded that the normal elevator control could be satisfactorarily maintained within the present speed range but that the drag rise due to control operation is greater than with an all moving tailplane.

Introduction

The object of the present tests was to supply data on the effectiveness of elevator control at supersonic speeds. In a previous experiment by the author[1] (1944) an EC 1240 section was used, as it was immediately available, but for the present tests a more suitable supersonic aerofoil was constructed. The previous experiments had shown C_L and C_m to be linear with α and η and this was supported by theory. For the present work two models were used, one a symmetrical double wedge 0.06c thick and the other of the same basic section with the portion aft of the 0.7c line depressed 4 deg. (Fig.1). The force-coefficient slope against η was calculated from the difference between the forces on the two sections.

The tests were carried out on the electric balance of the 12 in. circular wind tunnel. The wind tunnel nozzles had area ratios corresponding to 1.34a (nominal 1.2a) and 1.51 (nominal 1.4a) respectively. Other and varying speeds were obtained from day to day between 1.16a and 1.45a. It was hoped to obtain confirmation of the theoretical variation of force coefficients with

Mach/

'A' REPORT

Mach number within the test range. The tests also supplied data at speeds at which no theoretical analysis was possible. The value of these results is discussed later.

The model was also tested with its trailing edge into the wind, giving the effect of a leading edge flap.

<u>Experimental Details</u>

The models were two dimensional in that they completely spanned the stream. The effect of the wall junction is discussed under the heading of wind tunnel interference (Appendix II). The cross section of the models tested is shown in Fig. 1.

The balance was designed to read the 3 components, lift drag and quarter chord pitching moment, as moments about each of 3 lines parallel to the span of the aerofoil. From these moments (reduced to coefficients B_L, B_D, B_m) the force coefficients were calculated. This presumed that the conditions in the wind tunnel remained constant during the measurement of all 3 moments. In practice it was found impossible to maintain the velocity constant for readings on all 3 axes.

The velocity and Mach number was derived from the static pressure on the walls of the working section ahead of the model. The change of total head has been neglected. The tunnel speed measured in this way varied with atmospheric conditions. With the lower speed effuser (nominal 1.2a) speeds were obtained from 1.16a to 1.24a and from 1.37a to 1.45a with the higher speed effuser (nominal 1.4a).

H_2O depresses value of γ

It seems likely that this variation was largely due to condensation of moisture in the stream, the amount varying with the atmospheric humidity. The mechanism by which condensation affects the stream Mach number is not yet completely understood. For the purpose of the present paper it is sufficient to say that a heat release in a supersonic stream has the effect of varying the Mach number both gradually and through compression shocks. With changing humidity these shocks vary in amplitude and angle with a consequent alteration of the velocity and velocity distribution in the working section. Such a variation of distribution should show up as an incorrect indicated Mach number giving departures from smooth curves of forces as functions of Mach number.

B_m at zero η, was found to be comparatively insensitive to Mach number. As the Mach number changes between the tests on different axes were small, C_L and C_D are given as if B_m had been read at the same Mach number as the corresponding B_L or B_D. (See Appendix).

The wind direction was obtained from a comparison of the lift of the model tested normally and reversed end for end.

In the presentation of the results, advantage has been taken of symmetry, allowing the observations to be used twice whenever it occurred.

Observations were normally taken up to the highest incidences at which the velocity remained supersonic at the walls opposite the centre of the model. It is shown later that the model was then already subject to interference from the tunnel walls.

In view of the impossibility of calculation of the forces, measurements at $M = 1.16$ were continued even though the stream was subsonic in part and the observations subject to an unknown interference.

The/

The Reynolds number of the tests varied from 0.81 to 0.82 millions over the speed range.

Comparison with Theory

The force coefficients on a general two dimensional double wedge elevator combination were given by Loch[2] (1944). The basis of the calculation was the Busemann pressure relation between stream deviation and pressure. The formulae so derived are reproduced here for the particular case tested.

$$C_L = 2c_1\alpha + 0.6\eta\,(c_1 - 0.12c_2)$$

$$C_{m_{\frac{1}{4}}} = -0.5\alpha\,(c_1 - 0.12c_2) - 0.36\eta\,(c_1 - 0.12c_2)$$

$$C_D = 2c_1\,(\alpha^2 + 0.0036) + 0.6\eta\,(\eta + 2\alpha)(c_1 - 0.18c_2)$$

where α and η are in radians and c_1 and c_2 defined by

$$c_1 = 2/(M^2 - 1)^{\frac{1}{2}}$$

$$c_2 = (1.2M^4 - M^2 + 2)/(M^2 - 1)^2.$$

The following formulae, also due to Lock, were calculated by the same method[2] for the leading edge flap.

$$C_L = 2c_1\alpha + 0.6\eta\,(c_1 + 0.12c_2)$$

$$C_{m_{\frac{1}{4}}} = -0.5\alpha\,(c_1 - 0.12c_2) + 0.06\eta\,(c_1 + 0.12c_2)$$

$$C_D = 2c_1\,(\alpha^2 + 0.0036) + 0.6\eta\,(\eta + 2\alpha)(c_1 + 0.18c_2)$$

η was reckoned positive downwards for the normal elevator, and positive upwards for the leading edge elevator. In each case positive η angles produce positive lift. Wherever applicable these theoretical values are shown as dotted curves with the full lines of the observed values. The limits to the theory imposed by sonic speed being attained in the pressure field of the aerofoil are also shown in most figures. This limit to either Mach number or incidence has been called the critical Mach number or critical incidence in conformity with subsonic aerodynamic practice. They were derived from Meyer's[3] (1908) tables of Mach number and stream deviation for isentropic expansion of dry air. If a supersonic stream of Mach number M_1 is considered to have been expanded isentropically through an angle θ, from the state $M = 1$, $\theta = 0$, an isentropic compressive deviation of θ would decrease the local Mach number again to unity. Below $M = 1.6$, $\theta = 15$ deg. compressions can be regarded as isentropic. Hence for a given Mach number, Meyers' tables can be used to indicate the compressive deviation corresponding to sonic speed behind the resulting shock, within the above limits the critical Mach number is sufficiently nearly a function of the maximum inclination of the surfaces (towards the wind) only.

The probability of spanwise variation of velocity made these limits at best approximate. They provided however an indication of the onset of critical conditions. In some cases the theoretical curves have been extrapolated past the sonic limits as they were still in reasonable agreement with experiment.

Results/

U-3122

Results

(1) The Symmetrical Aerofoil. (Zero η)

Lift. - Figure 3 shows all the experimental results in the form of a C_L carpet for $\eta = 0$. The lift incidence slopes are shown in Figure 4. As the critical Mach number is approached the slope near zero incidence tends to exceed the theoretical value (Fig.4). The curve $M = 1.24$, $\eta = 0$ of Fig.3 shows an increase of slope beyond the theoretical value at incidences outside the range ±1 deg. (i.e. beyond the critical incidence). It must be stressed that the critical lines shown are not the sharp demarkation that the dotted lines would suggest due to the probability of varying velocity distribution across the span.

The fact that the slopes $\left(\frac{\partial C_L}{\partial \alpha}, \text{Fig.4}\right)$ for the flapped and unflapped aerofoil agree with each other as predicted by theory although neither has the true theoretical value, suggests a lack of homogeneity in the stream. Further evidence in favour of the theory was given by the better agreement of the observed and theoretical lifts as the tunnel speed approached its designed value, implying a greater freedom from shocks and hence a better velocity distribution in the working section. (Fig.4 $M = 1.38$ and 1.45).

The dotted parts of the curve $M = 1.16$ (Fig.3) refer to tests made with the velocity subsonic at the wall opposite the centre of the model on the compression side. They indicate that no violent change is to be expected as the critical incidence is passed. Owing to the constraint of the wind tunnel walls the actual value of the measured lift should be viewed with caution.

Pitching Moment. - The quarter chord pitching moment is presented in a similar manner to the lift, in Figures 5 and 6. As in the case of lift the dotted portion of curves $M = 1.15$ and $M = 1.16$ denotes subsonic speed at the wall of tunnel. Their continued linearity with α through $\alpha_{crit.}$ is interesting. It suggests that interference is either small or fairly fully developed below $\alpha_{crit.}$ (see Appendix I).

The scatter of Figure 6 was not unexpected and can be attributed to a varying velocity distribution (i.e. an error in indicated Mach number). Even allowing for such uncertainty the experimental points are all less negative than the theoretical.

Again the incidence slope of the two flapped aerofoils agreed reasonably well with the unflapped one, and this result is in accordance with theory.

Drag. - Figure 7 contains the whole of the experimental results of drag on the unflapped aerofoil. Figure 9 gives two specimen curves with the actual observations, to demonstrate the degree of scatter of the observations and the accuracy of the results. The corresponding theoretical curves are included for comparison. In Figure 7 advantage was taken of symmetry, allowing each observation to be used twice. Values at positive incidence only have been plotted for clarity.

Figures 9 and 11 together indicate that at the Reynolds number of the present tests (0.81×10^6) a skin friction drag coefficient of 0.004 is applicable. Here again stream irregularities prevent any definite statement, as included in this value in any force due to buoyancy. In an extreme case this could amount to -0.004 on C_D, giving $C_{D_F} = 0.008$ (German workers have quoted 0.006).

The/

The observations of curves 7 and 9 have been replotted against α^2 at constant M in Figure 12. Their linearity is in confirmation of theory. Their slopes, as a measure of wave drag are shown as a function of M in Figure 13. Too much weight should not be given to the point $M = 1.19$ in view of the very few points (Figures 7 and 12) determining the slope. The indication remains however that the wave drag rose to the critical Mach number and then fell again. There is a suspicion of a change of slope where the curve $M = 1.24$ of Figure 12 crosses the sonic line but this is insufficient evidence from which to draw any inference. It was unfortunate that this curve was the only one to include the critical angle in the incidence range.

Values of C_D are plotted against C_L (for $M = 1.38$) in Figure 18 for comparison with curves of the flapped aerofoil and are discussed later.

The probable effect on drag of tunnel wall interference is discussed in Appendix II.

(2) Results on Control Characteristics

Lift (Normal Elevator).- The results of Figure 3 have been combined in Figure 14. The value of $\left(\frac{\partial C_L}{\partial \eta}\right)_\alpha$ was obtained from the difference of C_L at $\eta = 4$ deg. and $\eta = 0$ deg. The agreement with theory is reasonable except for the sharp rise near the critical Mach number. Some of this rise, at least, can be attributed to interference from the tunnel walls. The fact that the experimental points are below the theoretical ($M = 1.38$ and 1.45) suggest a boundary layer separation on the top surface of the flap due to the trailing edge shock. (cf. Ferri[4] 1939).

Pitching Moment.- The experimental moment results support this suggestion. (Figure 15). Wind tunnel interference would have the effect of increasing the nose down pitching moment of the sections. The point at $M = 1.25$ is therefore much less negative than expected, which is in conformity with the idea of a separation on the upper surface and possibly in the re-entrant angle of the hinge.

Drag.- No simple presentation of the effect of α, η and M on drag was possible owing to the more complicated nature of their relation. Figures 8 and 10 show the drag at $\eta = 4$ deg. in the same way as Figures 7 and 9 did for $\eta = 0$. Each agreed with theory to the same order of accuracy.

Results at a Mach number of 1.38 for the three cases $\eta = 0$ deg. $\eta = 4$ deg. and $\eta = 4$ deg. (leading edge elevator) are plotted against lift coefficient in Figure 18 (curves E, F, and G) and compared with the corresponding theoretical values (B; C, and D); the agreement after allowance has been made for skin friction is again reasonably good. On the same figure are plotted (curves A and H) theoretical values of C_D for $\alpha = 0$ and varying η for the normal and leading edge elevation respectively. They show that the drag increased as a result of elevator operation is considerably greater than for an all moving tailplane.

Hinge Moment.- It was possible to calculate the hinge moment at $\alpha = 0$ of the flap from the variations of the pitching moment with η. Assuming that all changes of lift and moment on the aerofoil due to a movement η of the flap occurred as a change in normal force on the flap alone, the hinge moment is given by the pitching moment of the aerofoil about the hinge line of the flap. Giving

$$C_H = C_m + 0.45\ C_L .$$

This/

This implied that there was no boundary layer and that the flow everywhere followed the profile of the section. In view of the repeated indication of boundary layer effects this was somewhat dubious.

The experimental values of hinge moment on the normal elevator were less than those predicted by theory. (Figure 16). This was in conformity with the expected effects of a boundary layer. The change in sign of $\left(\frac{\partial C_H}{\partial \eta}\right)$ at low Mach numbers should not be regarded as a sign of an unstable stick force but merely that the normal reaction had left the flap, demonstrating the unreliability of the method.

The Leading Edge Elevator.- Results are available only at $M = 1.38$ as the supersonic regime could not be established with the lower speed effuser nozzle in place. (This may have been due to the relatively higher drag).

In both the case of C_L (Figure 4) and of C_m (Figure 6) the leading edge elevator is in very fair agreement with theory. The lift slope $\left(\frac{\partial C_L}{\partial \eta}\right)$ is roughly double that for the trailing edge flap, (Figure 14) but the moment changes (Figure 15) are considerably smaller than with a conventional control.

The hinge moment calculated in a similar manner to the previous case is

$$C_H = C_m + 0.05\ C_L.$$

Reasonable agreement with theory was obtained. (Figure 16). The curves indicate that the leading edge elevator is less influenced by the boundary layer making the prediction of full scale control more certain. Distortion of a wing or tailplane due to the forces on the flap cannot give control reversal with a leading edge flap. These advantages are offset by the fact that under all circumstances the leading edge flap gives rise to an unstable stick force. The drag for a given lift is higher than in the case of a conventional control. (Figures 18).

Conclusions

At Mach numbers about 1.4 the experimental evidence supports Busemann theory reasonably well. At lower Mach numbers deviation from the theoretical values was obtained. This could be attributed chiefly to interference from the walls of the wind tunnel and to bad velocity distribution in the empty tunnel.

The impossibility of using optical means of investigation made the interpretation of the majority of the phenoma a matter of conjecture. The authors experience in other wind tunnels and the work of Ferri[4 & 5] in Italy indicated that the boundary layer in the presence of shocks could supply a qualitatively satisfactory explanation for some of the discrepancies.

The broad indications are that both leading and trailing edge flaps produce reasonable control forces, but that the leading edge flap is unstable.

The variable incidence tailplane appears the most suitable method of control from the aerodynamic point of view, as its drag is lower for a given control force, and it is less sensitive to boundary layer effects, making the prediction of full scale forces more certain. A third reason, outside the scope of the present work, is that control is likely to be better with a moving tailplane at transonic speeds.

In/

In the interpretation and application to full scale, of the results considerable caution is advised.

References

1. F. W. Pruden : Tests of an aerofoil with a 40 per cent Hinged Flap at Supersonic Speed. (1944). 7615.

2. C. N. H. Lock : Examples of the Application of Busemann's Formula to Evaluate the Aerodynamic Force Coefficients on Supersonic Aerofoils. (1944). 8027.

3. Th. Meyer : Two Dimensional Flow Phenomena in Gas at Supersonic Speed. Forsch. Ing. Wos. 62. (1908). Reproduced in 3210 by O. Walchner (1937).

4. A. Ferri : Atti di Guidonia No.17. R.T.P. Translation 1115. (1939).

5. A. Ferri : Atti di Guidonia No.37. R.T.P. Translation 1407. (1940).

6. D. Holder and P. M. Burrows : Explorations along the Axis of Two Supersonic Wind Tunnels of the Injector Type. 8670.

Appendix I/

Appendix I

The Computation of Force Coefficients from B_L, B_D, B_m

B_L and B_m were sensibly linear with α through $\alpha = 0$ although departures were obtained at the lower Mach numbers. In order to obtain some insight into the correction necessary to B_m to obtain the coefficients C_L and C_D Figure 2 was plotted. ($C_L = B_L - B_m$, $C_D = B_D - \frac{1}{2} B_m$, $C_m = \frac{1}{2} B_m$, plus small corrections in each case). If the tunnel speed or distribution altered between the reading of the two moments B_L and B_m, the formulae no longer apply.

In Figure 2, $\frac{dB_L}{d\alpha}$ and $\frac{dB_m}{d\alpha}$ are plotted against Mach number for the case $\psi = 0$ and the theoretical curves are included for comparison. Busemann theory gave

$$B_L = \frac{\alpha}{57.3}(c_1 + 0.12\, c_2)$$

$$B_m = \frac{-\alpha}{57.3}(c_1 - 0.12\, c_2)$$

(α measured in degrees).

A number of significant points are immediately apparent. The lack of smoothness of $-\frac{dB_m}{d\alpha}$ when plotted against M was not unexpected. The smoothness of $\frac{dB_L}{d\alpha}$ was somewhat perplexing since B_L was the moment of the resultant force about the 0.75c line and B_m the moment about the 0.25c line. A possible explanation was given by the greater sensitivity of B_m to changes at the trailing edge. Boundary layer variations due to extraneous shocks might be expected to be worse at the trailing edge where the boundary layer was thicker. Another seeming paradox was the agreement between the theoretical and experimental values of $\frac{dB_L}{d\alpha}$ at $M = 1.37$ and the poor agreement of $\frac{dB_m}{d\alpha}$. This could be explained by considering both the calculated lift force and calculated centre of pressure to be different from the observed values by amounts which compensated in the product for B_L but not for B_m. Assuming such differences and substituting the values of $\frac{dB_L}{d\alpha}$ and $\frac{dB_m}{d\alpha}$ from Figure 2 two simultaneous equations were obtained from which were calculated the numerical differences between the observed and theoretical systems. They showed the measured lift slope to be 0.01 per degree low and the centre of pressure 0.04 chords further forward relative to the Busemann value.

In view of the scatter of B_m against M no correction was undertaken for change of M between readings on the 3 axes. C_L and C_D have been given as if B_m had been read at the same Mach number as the corresponding B_L or B_D.

Appendix II/

Appendix II

Wind Tunnel Interference

There are a number of ways in which a supposedly two dimensional supersonic stream can differ from free air conditions.

In a completely supersonic stream where striometric observations are possible the zones of interference are clearly visible and in two dimensions the interference pressures can be calculated. This is not sufficient however as the interference can either augment or suppress the boundary layer separation from the trailing edge, at least at the Reynolds number of the present test[4].

In the N.P.L. circular supersonic tunnel the Mach number at which interference commences (e.g. reflected waves touch the trailing edge) varies with the spanwise position. The reflected shock too, has a greater amplitude at the centre of the model. The model of the present experiment was subject to such interference at all speeds below $M = 1.25$ at $\alpha = 0$ deg. and correspondingly higher speeds at the higher incidences. The arrangement of the tunnel precluded any attempt at calculation, even ignoring boundary layer effects, but a qualitative estimate can be made. Reflected wave interference would be expected to give a spurious increase of lift accompanies by a movement aft of the centre of pressure (a nose down pitching moment). At small incidences the effect on drag should be small with the 6 per cent double wedge aerofoil, but reaching a maximum as the reflected wave passes the mid-chord line. When the incidence is sufficiently high to incline the rear face of the pressure side of the aerofoil to the stream, the interference acts in the sense of a positive drag.

The decrease of lift over the part of the span washed by the tunnel boundary layer is of small importance as the boundary layer is thin and the downwash gradient is limited to the Mach cones from the intersection of the aerofoil and the boundary layer.

An extraneous wave system would be introduced should the tunnel wall boundary layer separate due to the nose wave of the model. This would be the wave system of a swept back wedge in a plane perpendicular to the span of the model. Whilst the bow wave is at the Mach angle the separation wedge would be swept back at the same angle having a consequently negligible wave system, but as the amplitude of the bow wave increases so would the amplitude of the interference system and its area of influence.

In the present tests there was also an incalculable effect from the holes in the tunnel wall through which the aerofoil passed.

There was also a random error due to the changing irregularities of the stream. Typical examples have been quoted in an earlier report (Holder and Burrows[6] 1945). Such irregularities cause errors in the indicated Mach number and the spanwise force distribution with a further possibility of force modification due to local separations caused by extraneous shocks. An attempt was made by the author (unpublished 1944) to measure the total effect of the junction of model and wall at $M = 1.4$. Three model wings were used each of different span. The free end was cut off at such an angle as to eliminate induced tip effects and the other end supported in the balance, the wing passing through the wall in the normal manner. From the forces on the 3 wings of different span it should have been possible to calculate the end effects. Unfortunately the random errors introduced by stream irregularities masked the interference under investigation. Although these errors were large the results suggested that the interference at that speed was small. This is of course, not necessarily so at the lower Mach numbers.

The/

The total interference effects would appear to be an increase of lift and a movement aft of the centre of pressure as the critical Mach number is approached. The drag effect is more difficult to predict but at low incidences on the 6 per cent double wedge an increase in drag might be expected reaching a maximum as the reflected waves move up to the half chord line. At higher incidences a decrease in drag is possible but on the whole the drag errors should be small.

Stream irregularities giving rise to buoyancy forces have been discussed earlier in the text.

Appendix III

A Comparison of Three Forms of Control

1. The moving tailplane
2. The trailing edge hinged flap
3. The leading edge hinged flap.

In the following simple analysis comparison is made on a basis of the drag of the tailplane unit, to produce a given lift. In each case the basic tailplane section has been taken to be a symmetrical double wedge of semi-angle β.

Busemann's approximation gives

1. All moving tailplane ($\eta = 0$, α varying)

$$C_{D_1} = 2\, c_1\, \beta^2 + \frac{C_L^2}{2\, c_1}.$$

2. Trailing edge elevator flap (flap chord E) ($\alpha = 0$, η varying)

$$C_{D_2} = 2\, c_1\, \beta^2 + \frac{C_L^2}{2E}\,\frac{(c_1 - 3\beta c_2)}{(c_1 - 2\beta c_2)^2}.$$

3. Leading edge elevator flap ($\alpha = 0$, η varying)

$$C_{D_3} = 2\, c_1\, \beta^2 + \frac{C_L^2}{2E}\,\frac{c_1 + 3\beta c_2}{(c_1 + 2\beta c_2)^2}.$$

In each case a skin friction drag coefficient should be added but the experiment suggests that it is sufficiently constant in the three cases to be neglected in the comparison.

The condition that C_{D_2} is greater than C_{D_1} at a given C_L now becomes

$$\frac{1}{c_1} < \frac{1}{E}\,\frac{c_1 - 3\beta c_2}{(c_1 - 2\beta c_2)^2}.$$

(Always with the proviso that β, and C_L (as a function of η) lie within the limits imposed by sonic velocity being reached).

The/

The complete solution of these simultaneous inequalities could be made by graphical means. In view of the labour involved it was thought preferable in this case to evaluate the conditions for the sections tested ($E = 0.3$), giving

$$\frac{c_1}{\beta c_2} > 3.12.$$

Within the theoretical limits this is always true. Therefore such a moving tailplane is superior from the considerations of drag, at all Mach numbers to which the theory applies.

In Figure 18(b) the experimental curves are compared with the theoretical curves of C_D, C_L at $M = 1.38$. There are shown also the theoretical curves for a tailplane elevator combination at $\alpha = 0$, (with η varying) for both a leading and trailing edge flap. (Figure 18(a)). The superiority of the moving tailplane is demonstrated (cf curves B, A and H). Curves C and E can also be regarded as a particular case of a cambered tailplane.

An interesting point to note, is that although $\left(\frac{\partial C_L}{\partial \eta}\right)_\alpha$ is less for the trailing edge elevator than the leading edge, the trailing edge elevator can produce a higher C_L within the sonic limits. This is due to the fact that the expansion round the mid-chord angle raises the velocity over the rear half of the aerofoil allowing a bigger maximum compressive deviation (actually 2β larger). The sketches of Figure 17 demonstrate this. In each section of the pressure field, θ gives the equivalent angular expansion from unit Mach number and hence the maximum permissible compressive deviation in that section.

A practical comparison must take into account the movement of the centre of pressure with lift and the change in the moment of the drag about the centre of gravity of the machine. This could be done for a general wing-tailplane combination, but the absence of a body, the unpredictable performance of a tailplane elevator of finite span, and the uncertainty of scale effects make such a calculation so far from the practical case that it can be of little interest.

The deciding factor must remain the effectiveness of control at those Mach numbers near $M = 1$ where no theory applies.

NH

8960.
FIGS. 1 & 2.

FIG. 1.

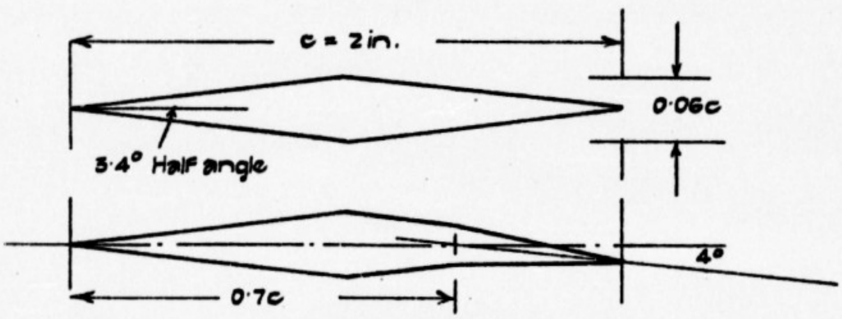

The Aerofoil Sections.
(not to scale).

FIG. 2.

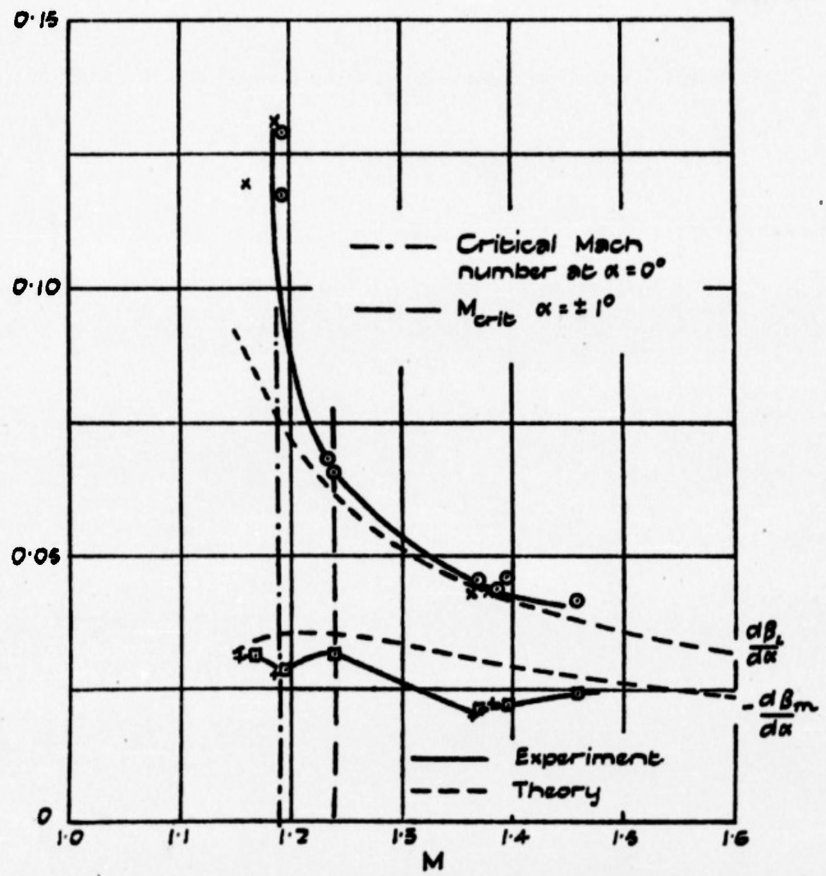

Variation of the Balance Coefficients with Mach Number ($\eta = 0$) α in degrees.

O.T.

(13)

8960.
FIG. 3.

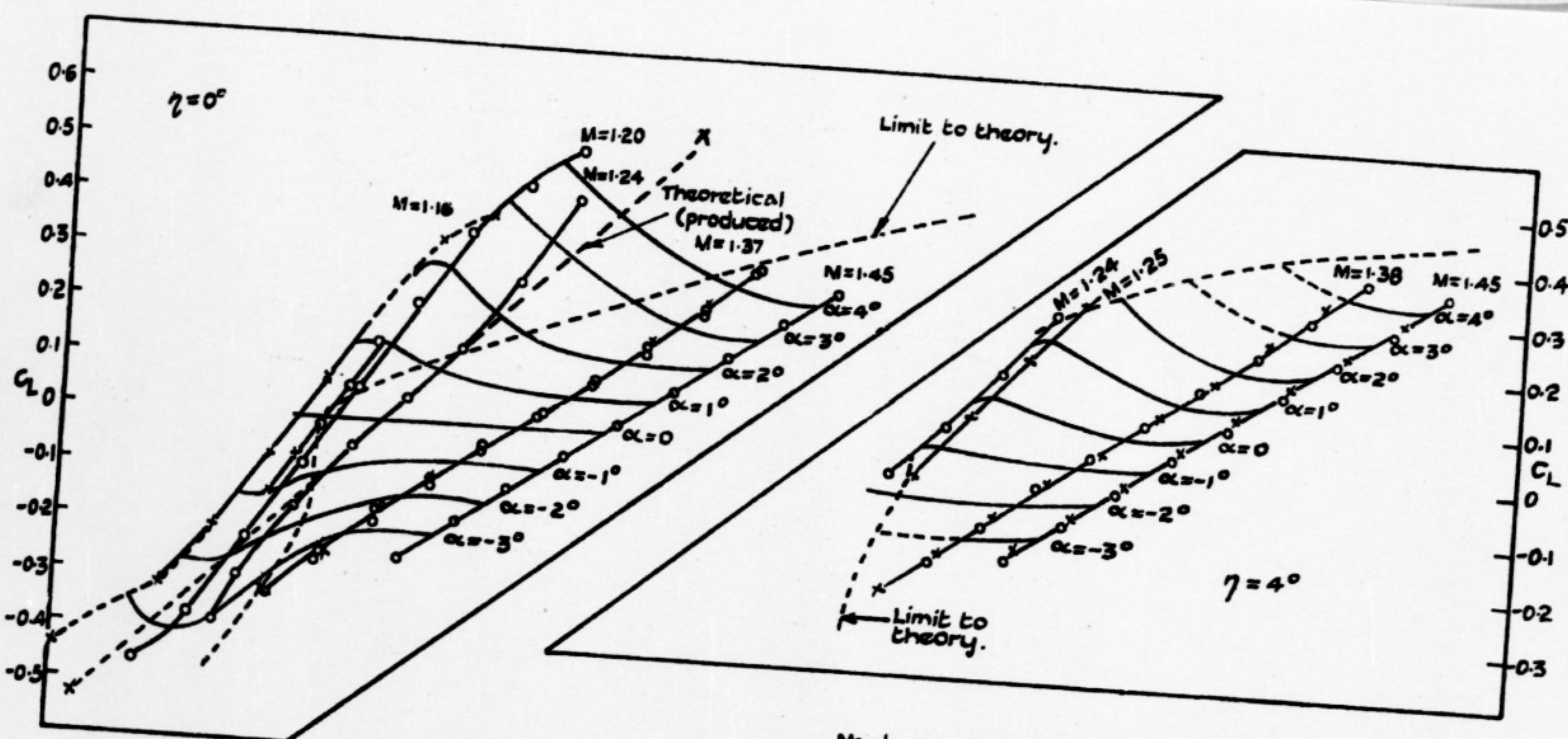

Mach number scale 2 cm = 0.1
Incidence 1 cm = 1

The variation of C_L with α, η, and M (normal elevator).

V.S.

(14)

8960.
FIGS. 4 & 6.

FIG. 4.

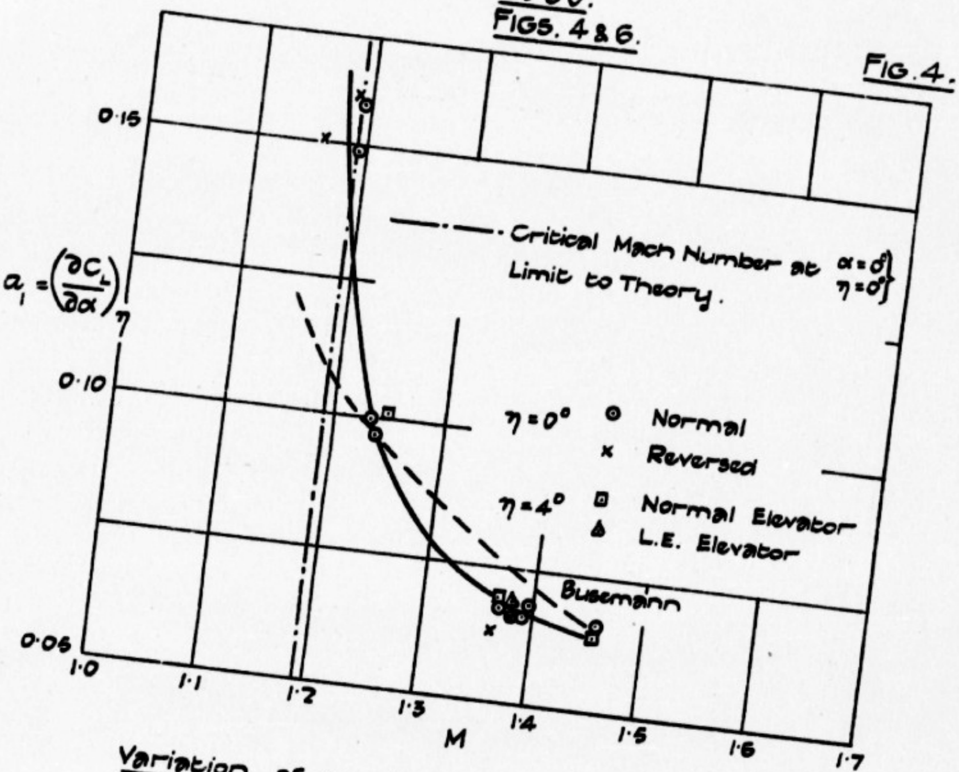

Variation of a_1 with M. (α in degrees).

FIG. 6.

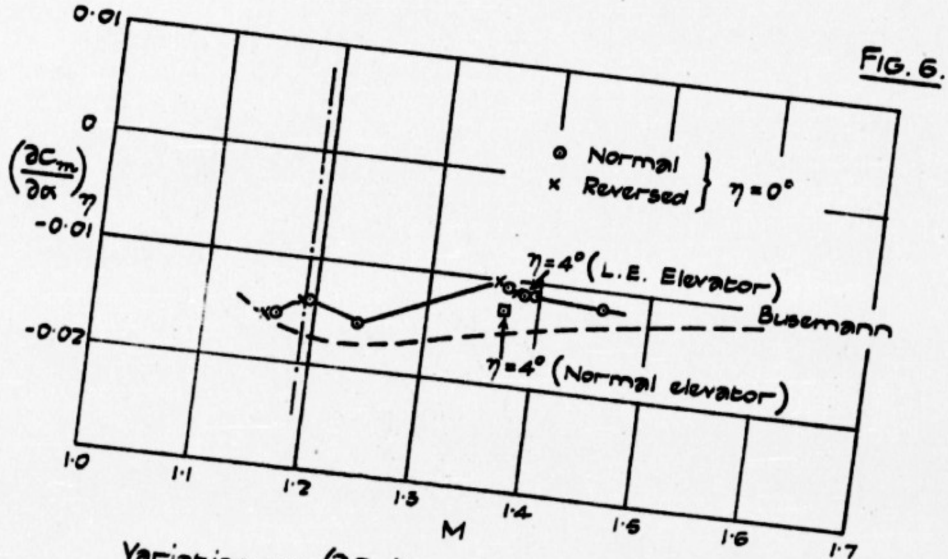

Variation of $\left(\frac{\partial C_m}{\partial \alpha}\right)_\eta$ with M. (α in degrees).

O.T.

(15)

8960.
FIG. 5.

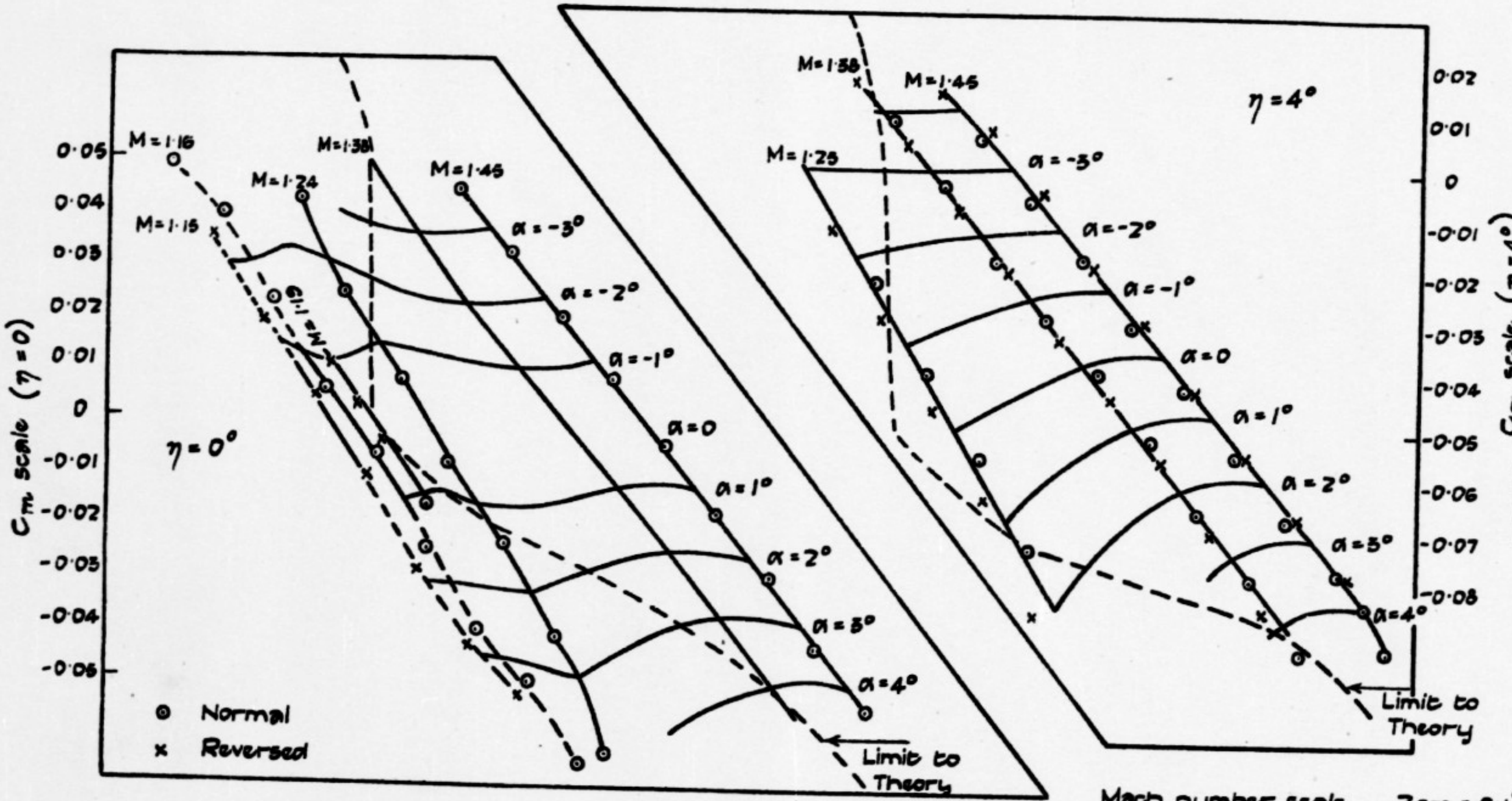

Mach number scale 2cm = 0·1°
Incidence scale 1cm = 1°

The Variation of C_m with α, η and M (normal elevator).

O.T.

FIG. 7.

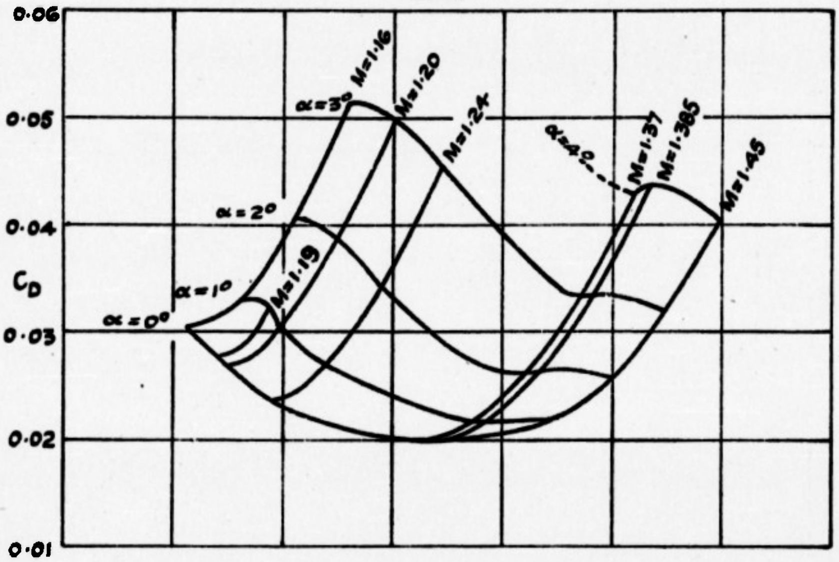

Variation of C_D with α and M at $\eta = 0°$.

FIG. 8.

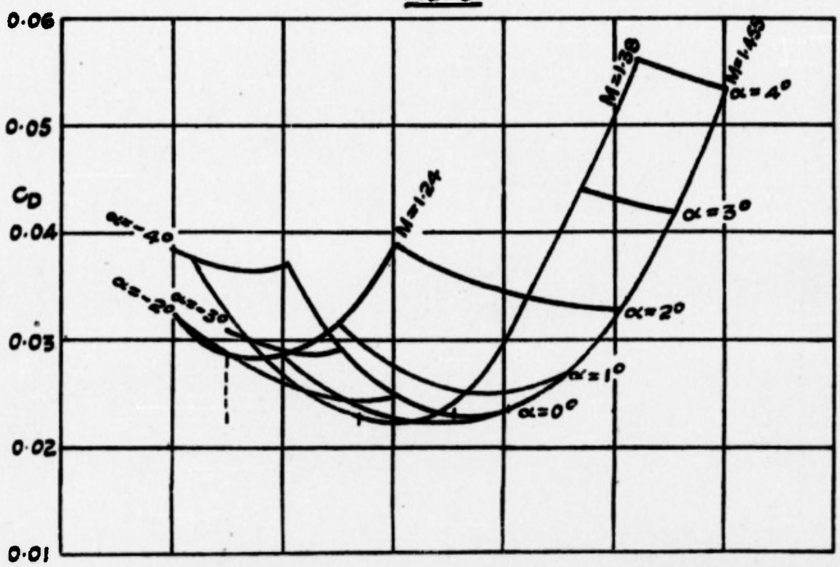

Variation of C_D with α and M at $\eta = 4°$.

(17)

8960.
Figs. 9 & 10.

Fig. 9.

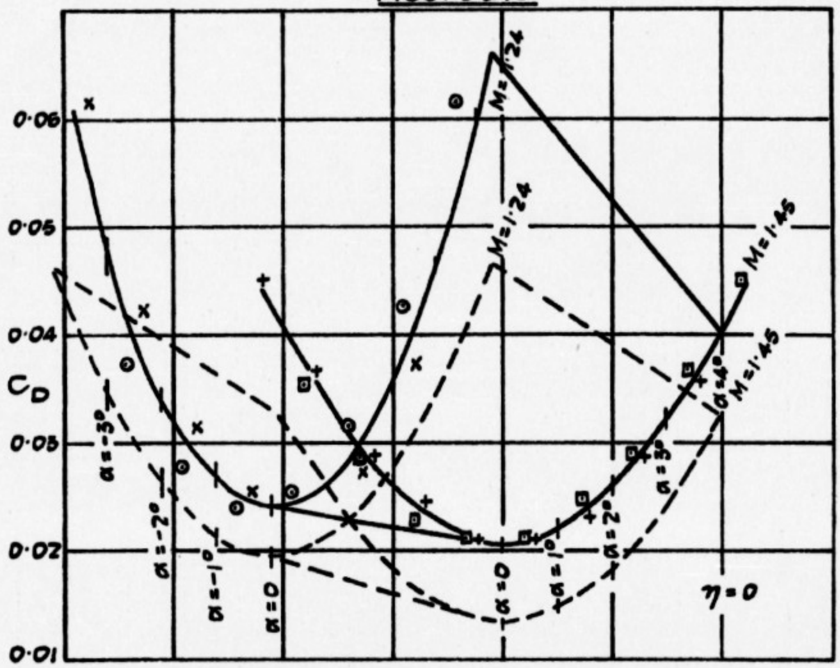

Comparison of Observed and Theoretical Drag at $\eta = 0$.

Fig. 10.

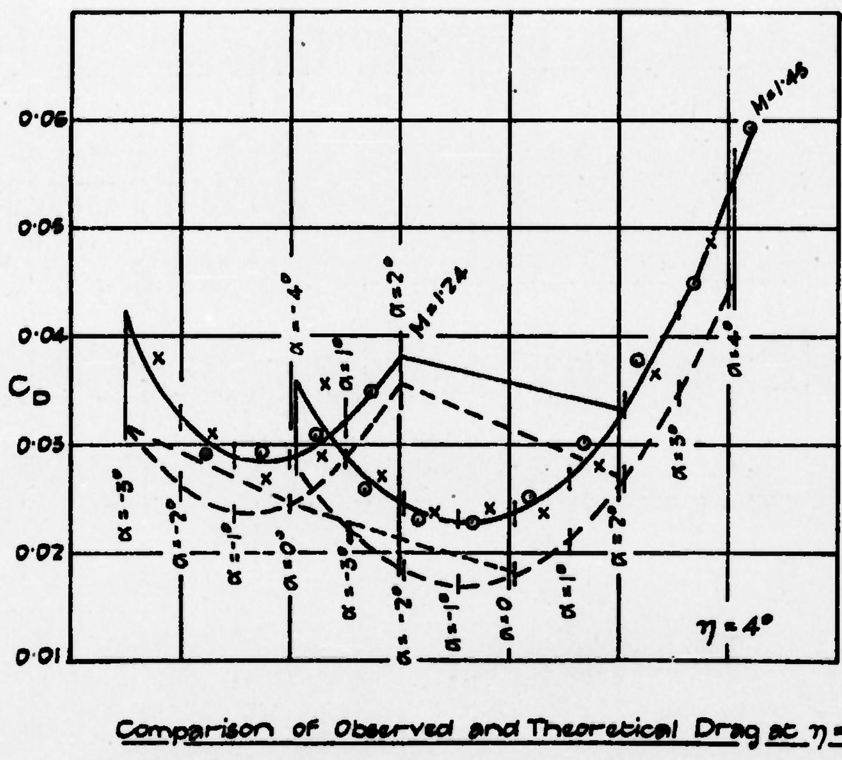

Comparison of Observed and Theoretical Drag at $\eta = 4°$.

G.T.

8960.

FIGS. 11-13.

FIG. 11.

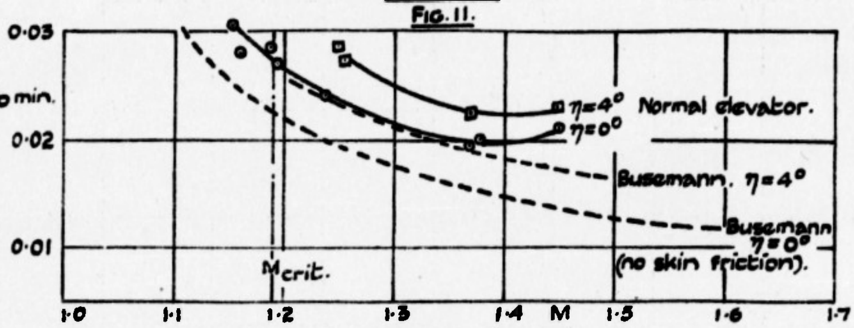

Variation of minimum C_D with M.

FIG. 12.

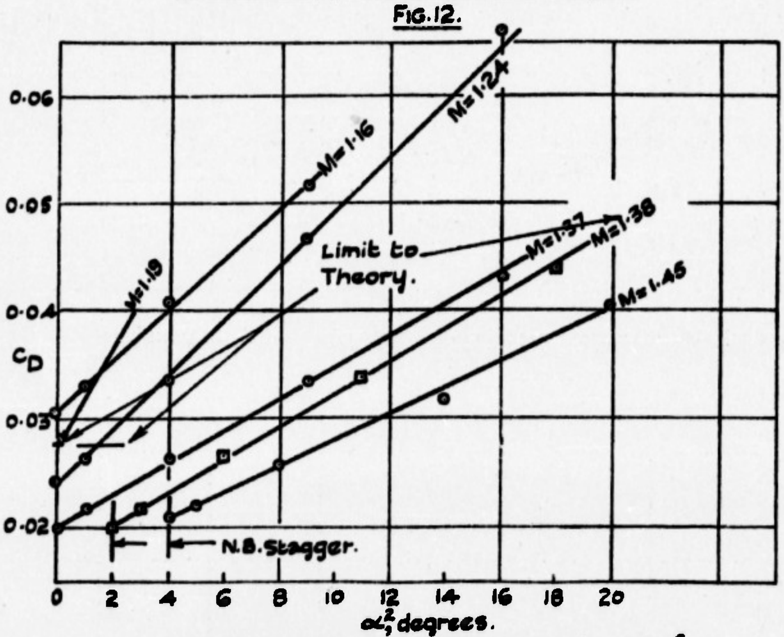

Drag as a function of incidence^2 ($\eta = 0°$).

FIG. 13.

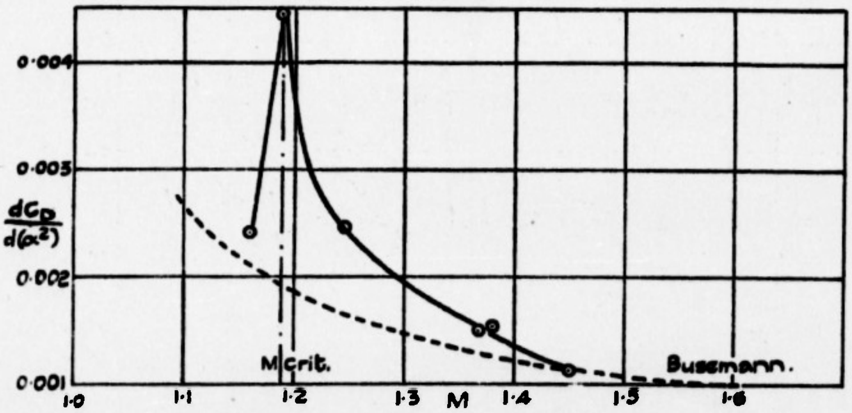

Wave drag as a function of M (α in degrees).

V.S.

Fig. 14.

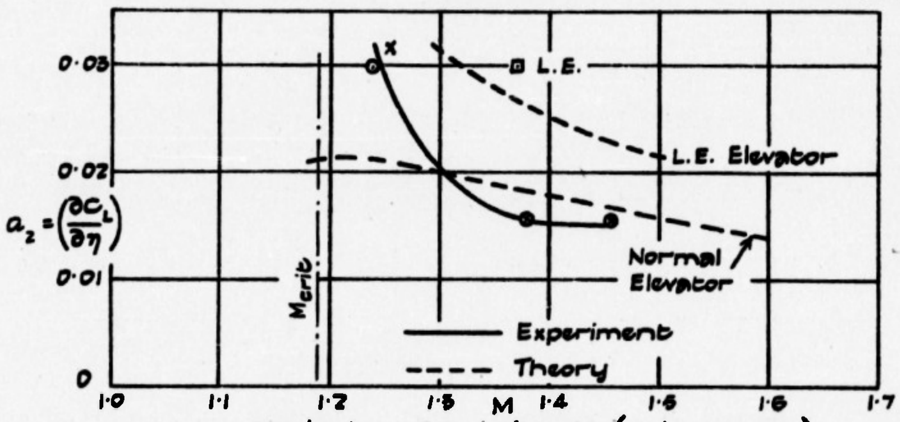

Variation of a_2 with M (η in degrees).

Fig. 15.

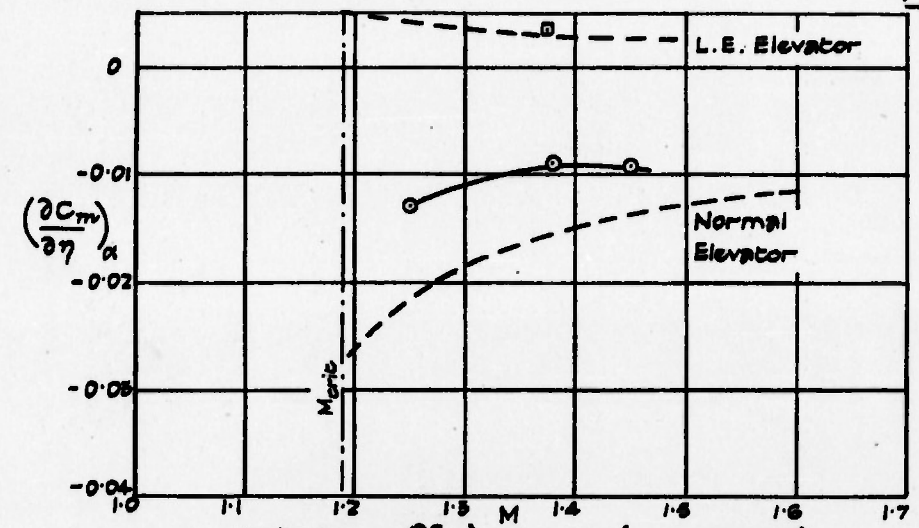

Variation of $\left(\frac{\partial C_m}{\partial \eta}\right)_\alpha$ with M (η in degrees).

Fig. 16.

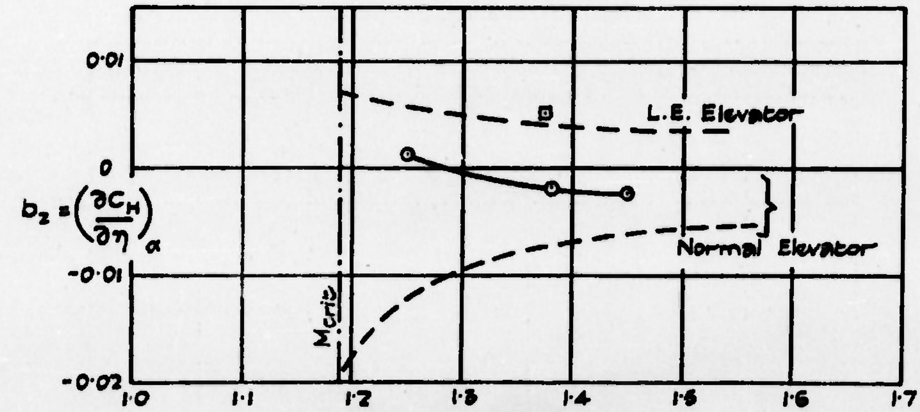

Variation of b_2 with M (η in degrees).
b_2 derived from C_m and C_L.

D.T.

8960.
Figs. 17, 18a & 18b.

Fig. 17.

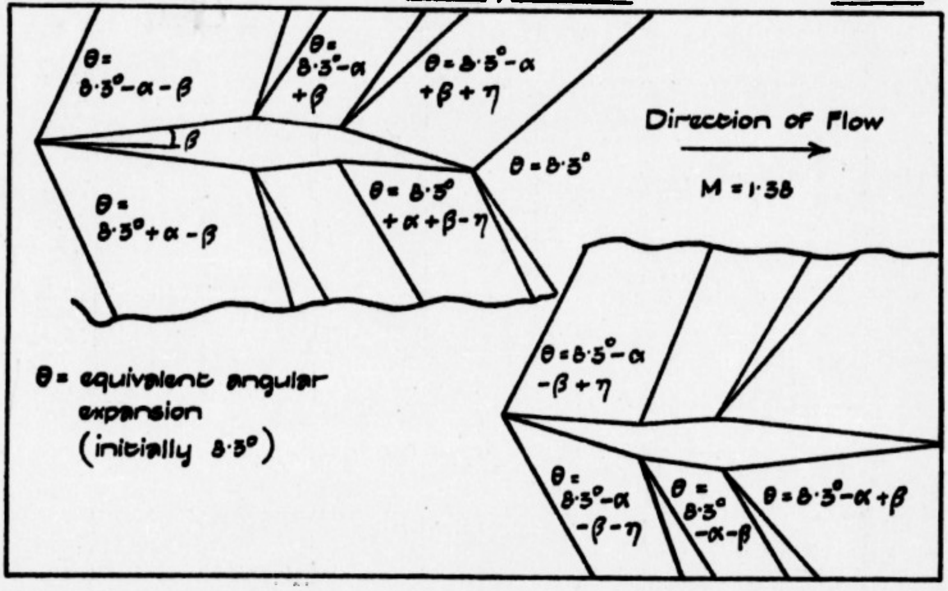

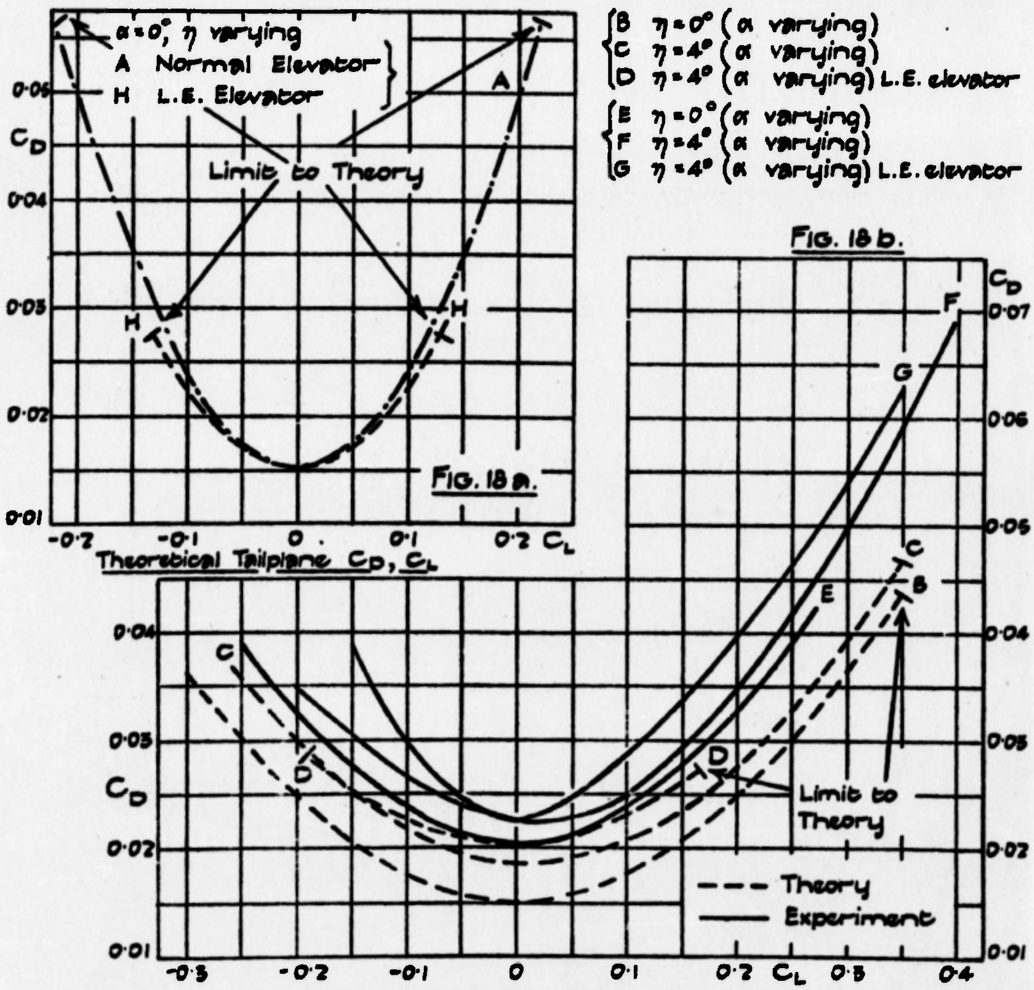

A Comparison of the Drag for the 3 types of Control.

O.T.

REEL - C

150

6212

TSDIO FORM 8 (10 FEB 47)

Pruden, F. W.

AUTHOR(S)

CONFIDENTIAL

C-2-6-32

DIVISION: Aerodynamics (2)

SECTION: Wings and Airfoils (6)

CROSS REFERENCES: Airfoil theory - Two dimensional (07200); Airfoils - Drag (08200); Wings - Pitching moment characteristics (99173.8)

ATI- 6212

ORIG. AGENCY NUMBER

R-8960

REVISION

AMER. TITLE: Tests of a double wedge aerofoil with a 30 percent control flap over a range of supersonic speeds

FORG'N. TITLE:

ORIGINATING AGENCY: Aeronautical Research Council, London

TRANSLATION:

COUNTRY	LANGUAGE	FORG'N.CLASS	U. S.CLASS.	DATE	PAGES	ILLUS.	FEATURES
Gt. Brit.	Eng.	Confd'l	Confd'l	Sep'45	20	16	graphs

ABSTRACT

Supersonic tests were conducted on a two-dimensional, symmetrical, double-wedge airfoil 6% thick with 30% control flap set at 4° and 0°. Results agree reasonably with Busemann theory. Lift, drag, and pitching moment were measured over Mach range of 1.16 to 1.45. Normal elevator control could be satisfactorily maintained within present speed range, but drag rise caused by control operation was greater than with variable incidence tailplane.

T-2, HQ., AIR MATERIEL COMMAND

AIR TECHNICAL INDEX

CONFIDENTIAL

WRIGHT FIELD, OHIO, USAAF

p 1 / /

23 * Aeronautical Engineering

25 * Airfoils

SHAPE

AERODYNAMIC CHARACTERISTICS

26 C

30 Aeronautical Research

WDIO FORM 0 B (10 52 47)

Pruden, F. W.

AUTHOR(S)

CONFIDENTIAL

C-2-6-32

DIVISION: Aerodynamics (2)
SECTION: Wings and Airfoils (6)
CROSS REFERENCES: Airfoil theory - Two dimensional (07200); Airfoils - Drag (08200); Wings - Pitching moment characteristics (99173.8)

ATI- 6212

ORIG. AGENCY NUMBER

R-8960

REVISION

AMER. TITLE: Tests of a double wedge aerofoil with a 30 percent control flap over a range of supersonic speeds

FORG'N. TITLE:

ORIGINATING AGENCY: Aeronautical Research Council, London

TRANSLATION:

COUNTRY	LANGUAGE	FORG'N.CLASS	U. S.CLASS.	DATE	PAGES	ILLUS.	FEATURES
Gt. Brit.	Eng.	Confd'l	Confd'l	Sep'45	20	16	graphs

ABSTRACT

Supersonic tests were conducted on a two-dimensional, symmetrical, double-wedge airfoil 6% thick with 30% control flap set at 4° and 0°. Results agree reasonably with Busemann theory. Lift, drag, and pitching moment were measured over Mach range of 1.16 to 1.45. Normal elevator control could be satisfactorily maintained within present speed range, but drag rise caused by control operation was greater than with variable incidence tailplane.

T-2, HQ., AIR MATERIEL COMMAND

AIR TECHNICAL INDEX

WRIGHT FIELD, OHIO, USAAF

CONFIDENTIAL

[dstl]

Defense Technical Information Center (DTIC)
8725 John J. Kingman Road, Suit 0944
Fort Belvoir, VA 22060-6218
U.S.A.

AD#: ADA800690

Date of Search: 14 Oct 2009

Record Summary: DSIR 23/14797
Title: Double wedge aerofoil with 30% control flap over range of supersonic speeds: tests
Availability Open Document, Open Description, Normal Closure before FOI Act: 30 years
Former reference (Department): 8960
Held by The National Archives, Kew

This document is now available at the National Archives, Kew, Surrey, United Kingdom.

DTIC has checked the National Archives Catalogue website (http://www.nationalarchives.gov.uk) and found the document is available and releasable to the public.

Access to UK public records is governed by statute, namely the Public Records Act, 1958, and the Public Records Act, 1967.
The document has been released under the 30 year rule.
(The vast majority of records selected for permanent preservation are made available to the public when they are 30 years old. This is commonly referred to as the 30 year rule and was established by the Public Records Act of 1967).

This document may be treated as UNLIMITED.